ELECTROCHEMICAL QUANTIFICATION OF DNA USING ALUMINUM OXIDE MEMBRANES

by

Rohit Sharma

A thesis submitted to the faculty of
The University of Utah
in partial fulfillment of the requirements for the degree of

Master of Science

Department of Mechanical Engineering

The University of Utah

May 2013

The University of Utah Graduate School

STATEMENT OF THESIS APPROVAL

The thesis of **Rohit Sharma**

has been approved by the following supervisory committee members:

Bruce Gale	, Chair	**10/23/2012** Date Approved
Stacy Bamberg	, Member	**01/15/2013** Date Approved
Florian Solzbacher	, Member	Date Approved

and by **Timothy Ameel**, Chair of the Department of **Mechanical Engineering**

and by Donna M. White, Interim Dean of The Graduate School.

ABSTRACT

DNA extraction automation is a major concern in molecular diagnostics where processing of numerous and daily samples of blood represent a labor-intensive task and are difficult to automate. With the rapid growth in the area of DNA diagnostics, there is an urgent need for the development of a microsized total analysis system which can perform all three of the primary tasks of nucleic acid-based diagnostics on a single chip: sample preparation, extraction of the DNA, detection and quantification. This thesis work presents design and fabrication of an integrated system that can extract and electrochemically quantify DNA simultaneously from any unknown sample on a single chip. The system is fabricated using aluminum oxide membranes as substrates for the extraction and quantification of DNA, bonded with the PDMS (Polydimethylsiloxane), whose layer provides the microfluidic inlet and outlet. Cost effective fabrication tools, such as Xurography (a knife plotter) and soft lithography, are used to obtain integrated hybrid fluidic and detector prototypes.

Characterization of the DNA quantification system is performed based on several important operational parameters such as different concentrations of gDNA (sample), voltage applied to the electrochemical detector, flow rate of the sample and carrier buffer and channel gap size between the detector electrodes. Three experiments with different experimental setup are applied to quantify the binding of DNA with the surface of

aluminum oxide membranes. The change in the current through the detector wires is found to be linear with different concentrations of gDNA. Using these experimental data, a calibration curve is obtained through which concentration and mass of gDNA that is extracted from an unknown sample can be determined successfully. This system thus provides us with several advantages, such as simultaneous extraction and quantification of gDNA, low detection limit of DNA (3.3ng/μL), low sample volume (200μL), high sensitivity and selectivity, low cost, small size, easy fabrication, portability, and disposability, when compared to other quantification systems.

TABLE OF CONTENTS

LIST OF TABLES

Table Page

LIST OF FIGURES

ACKNOWLEDGMENTS

Firstly, I would like to thank my advisor, Dr. Bruce Gale, for creating a discursive space in this discipline and taking special care to nurture this area of engineering. His timely conceptual and critical inputs along with his extended patience to accommodate me in his lab for conducting the experiments with my obsessive revisions virtually 'made' the book with me.

To my superiors, Dr. Himanshu Sant and Dr. Jungkyu Kim, for their extensive help during the course of the project, I express my thanks. I also thank my advisory committee members, Dr. Florian Solzbacher and Dr. Stacy Bamberg, for their occasional guidance and invaluable instructions. I am grateful to the State of Utah Center of Excellence for Biomedical Microfluidics which made my research possible and provided me with the financial support for this project. My special thanks to my very dear friends, Neha Berlia, Hannwelm Steinebach, and Tyagrajan Swaminathan, for their constant support and encouragement.

And above all, to my parents for their unconditional support, I am forever indebted.

CHAPTER 1

INTRODUCTION

Analysis of deoxyribonucleic acid (DNA) has become a very crucial and versatile tool for genetic diagnostics. The development and growth in the field of BIO-MEMS (micro electromechanical systems) and microfluidics has revolutionized the capabilities of researchers in the area of genomics and clinical diagnostics. In the year 1990, when the concept of a *micro total analysis system* (μTAS) was first proposed by Manz, *et al.* [1], the first successful integration of solid phase extraction (SPE), polymerase chain reaction (PCR), and microchip electrophoresis, onto a single device was completed, with the capability of sample-in/answer out in 25 minutes. Over the past two decades, the area of μTAS, alternately named "Lab On a Chip" (LOC) has gained tremendously in importance and has experienced rapid growth. According to a market analysis, the European LOC and microfluidics market have together generated revenue of about $666.3 million in 2008 and, by the year 2015, this is estimated to reach $1.62 billion [2]. With the tremendous growth potential in this area, the trend is certainly in favor of miniaturization in the fields of genomics, proteomics and clinical diagnostics.

Since the mid 1990's the μTAS technologies have exploded all across the world for biological sample analyses, chemical reactions, and diagnostics [3]. Low fluid volume consumption, faster analysis and response time, low fabrication costs leading to

disposability, and compactness of the system are among a few of the benefits duly recognized to be significant.

Effective extraction and detection of biological molecules, for example, the extraction of DNA/RNA from blood cells, has become a core subject of interest for many researchers in the field of biology and life sciences. A variety of microfluidic DNA extraction approaches have already been developed based on different methods, such as those using silica beads [4], nanoporous membranes [5], magnetic silica particles [6], and chitosan-coated surfaces [7]. Out of these adopted procedures, nanoporous aluminum oxide membranes integrated with a microfluidic system has shown great results for extraction of gDNA from lysed whole blood [8].

Currently, detection and quantification of DNA is usually done by fluorescence detection, which has become a widely used technique in both laboratory scale and high-throughput genomic research [9]. However, electrochemical detection of DNA, when compared with optical detection, such as that of fluorescence detection, offers remarkable advantages such as: high sensitivity and selectivity, low cost, portability, label-free DNA detection, low-power requirements and miniaturization [10].

Despite substantial development in micro/nanofabrication technologies, there still exists the need for a microfluidic integrated system which can provide extraction, detection, and quantification of a genomic sample, like DNA, on one single chip.

1.1. Micro-Chip Based Detection Methods

The combination of microfluidics and lab on a chip, in the area of sensitive molecular detection, promises the production of small and low-cost analysis systems with

improved sensitivity and selectivity, lower detection limits, and real-time analysis with ever-decreasing sample volumes. Notwithstanding the increased growth and development of microchip-based technologies over the last ten years, advances in effective and suitable detector systems for the detection and quantification of biological molecules has always lagged behind those of other process steps in the analysis of DNA [11].

To date, different modes of detection based on various detection concepts have been implemented for DNA analysis. All these concepts, and different methods based on these particular concepts, have been broadly classified in Figure 1.1.

The ultimate purpose behind this thesis is to design and fabricate a system that can extract unlabeled DNA using an aluminum oxide membrane (AOM) and simultaneously quantify the concentration of the DNA on the same chip. The main focus of this thesis will be on the detection and quantification of DNA using AOMs, as extraction of DNA using AOMs had been previously conducted successfully by our research group [12]. So far, many research groups have reported several detector systems for the detection of DNA using different detection concepts and principles. All these methods can be broadly distributed into two categories: *labeling methods* and *label-free methods*. The following section will serve as an overview of the various detector systems for detection and quantification of DNA that have been reported in the literature, featuring the optical, mass spectrometry and electrochemical readouts.

1.1.1. Optical Detection Systems

Optical detection of DNA and other biomolecules has found success employing laser-induced fluorescence (LIF) [13] and frequency modulated absorption. In LIF, DNA

is detected with the use of fluorescent labeling [14], which has also been the most commonly used detection system for microchip-based applications. LIF detectors come with the advantage of high sensitivity and selectivity. Unfortunately, these are very expensive and the process is time consuming, though the use of the required bulky off-chip control instrumentation is suitable for analytes that are naturally fluorescent, or molecules such as DNA that can be made highly fluorescent. The first fluorescence-based detector system was reported in 1995 by Krull [15]. This particular group used ethidium bromide as the indicator for DNA hybridization on optical fibers. Another group developed an on-chip fluorescence detector structure which uses a PINN+ photodiode with an interference filter and a robust liquid barrier layer [16]. With the application of photodiodes for DNA analysis, DNA was detected with a limit of 0.9 ng/μL using this system. Wolfgang Fritzsche, *et al.* [17], adopted the nanoparticle-labeling technique from microscope-based applications for DNA-chip detection.

With advantages like low background and high signal-to-noise ratios, and the other flexible properties of fluorescence such as wavelength and intensity, fluorescence-based detection methods are still dominating the field of detection for DNA analysis. However, other factors such as the bulky control instrumentation, large sample requirements, and their high cost, tend to limit their miniaturization and portability.

Another interesting optics-based detection technique is Surface Plasmon Resonance (SPR), in which label-free DNA can be detected. SPR-based sensors function by applying the principles of measuring the intensity [18], the resonant angle [19], and the wavelength of the reflected light [20]. One research group has shown work which focuses on dye-labeled DNA detection, using SPR-enhanced fluorescence readout [21].

Surface enhanced Raman spectroscopy (SERS) has also grabbed some attention for detection of biomolecules like DNA/RNA [22]. SERS is based on a surface-sensitive technique that can detect the enhancement in Raman scattering when molecules are adsorbed onto rough metal surfaces. Though providing high sensitivity and selectivity, the imaging system used in the sensors just discussed is prohibitively expensive and complex, limiting their application in μTAS.

1.1.2. Mass-Sensitive Detection Techniques

Biomolecules have been detected and quantified in terms of their mechanical response to external forces. Different biomolecules like DNA/RNA, proteins, etc., are probed with the application of external force using such tools as optical tweezers [23] and magnetic beads [24]. Another approach in this area was reported by Lang, *et al.* in which they used direct transduction of DNA hybridization via surface stress changes into the displacement of microfabricated cantilevers, thus eliminating the need of labeling the DNA with fluorescent or radioactive tags. Adopting the same principle, another research group has achieved high-sensitivity DNA detection by fabricating an array of 33 micro cantilevers with SU-8 [25].

In these mass-based sensors, the transduction of DNA recognition or any other molecular recognition into a nanomechanical response is achieved by immobilizing a monolayer of receptor molecules on one side of the cantilevers and then detecting the mechanical bending induced by ligand binding in a liquid environment. Mass-sensitive detection sensors eliminate the need of using labeled DNA and bulky control instrumentation, and they are small and portable; however, the fabrication process for

making these kinds of sensors is very convoluted and relies on classical photolithography techniques.

1.1.3. Electrochemical Detection Systems

For the last two decades, a wide range of electrochemical sensors for the detection of DNA have come to life and they continue to be an exciting field of research. The basic principle of an electrochemical detector system is to couple the biological recognition element (e.g., that of a DNA base-pair) to an electrode transducer, which then converts this particular recognition event to a useful electrical signal. These electrical signals, which can be in the form of current, voltage or impedance, can be measured to a fairly low limit, thus making a low detection limit for biomolecules feasible. Electrochemical sensors offer remarkable sensitivity and selectivity, without the rigorous sample-processing requirement of optical detector systems, label-free detection, low cost, simplicity, and portability, along with the inherent miniaturization of both the detector and control instrumentation. Thus, these sensors can be produced in mass quantities and be affordably disposable.

The history of electrochemical sensors for detection of DNA goes back to 1960, when Palecek first monitored the electrical activity of DNA by using oscillographic polarography with the application of mercury electrodes [26]. In another innovative approach, DNA oxidation was carried out through adsorption stripping voltammetry [27]. Since then, many other methods using silicon chips [28] and glass chips [29] as substrate for electrical detection of DNA have been discovered.

Electrochemical sensors can be divided into subcategories according to the electrochemical measurement technique used. These include measurement of current (amperometric sensors), current-voltage profile (voltammetric sensors), and voltage (potentiometric sensors). Amperometric and voltammetric sensors are most commonly used for detection and quantification of DNA. Their basic principle, advantages, and some of the state-of the art work done in this field are discussed next.

1.1.3.1. Amperometric Sensors

In amperometric sensors, a constant potential is applied across the working electrodes and the current associated with the reduction or oxidation of an electroactive molecule, involved in the recognition process, is monitored. In 1998, Wooley, *et al.* carried out the first electrochemical detection of DNA on a glass chip, which was based on amperometric measurement, using integrated working and counter electrodes [30]. The working electrode was placed using photolithographic techniques just outside the exit of an electrophoresis channel, providing high sensitivity, while the reference electrode used was in the form of an Ag/AgCl wire. In related work, gold microelectrode surfaces were used for carrying out enzyme-based amperometric detection of DNA [31].

The numerous advantages of using electrochemical sensors based on amperometric detection include minimal dead volume, wide linear range, short response time, preparation of electrodes that can be miniaturized to both micro and nanoscale, and the method is also compatible with planar micromachining technology.

1.1.3.2. Voltammetric Sensors

In voltammetric sensors, current is measured as a function of applied voltage which is swept over a range [32]. For electrochemical detection, usually two kinds of voltammetry, namely linear scan voltammetry and cyclic voltammetry are used. In cyclic voltammetry an alternating triangular-wave voltage is applied at a fixed scan rate to the working electrode, in a three-electrode cell setup, whereas a linear potential ramp is applied for linear scan voltammetry. As discussed before, Palecek in 1988 performed DNA oxidation using adsorption stripping voltammetry. By using this technique, direct nucleic acid reduction was observed and the single- and double-stranded DNA were discriminated. More recently, a novel electrochemical sensor based on dynamic polymerase-extending hybridization for the detection of DNA was demonstrated [33] by the use of cyclic voltammetry, while in another study the catalytic square wave voltammetric detection of DNA was achieved with use of pyrolytic graphite electrodes [34].

1.1.3.3. Potentiometric Sensors

In potentiometric sensors, the molecular recognition process is converted into a potential signal, by which means the species of the analyte is obtained in connection with the use of ion-selective electrodes (ISE). With tremendous improvements in the performance of ISE, it has now been demonstrated successfully that potentiometric sensors can be made small, portable, with low detection limit, and allowing measurements of very small sample volumes [35]. Numnuam, *et al.* demonstrated

potentiometric nucleic acid measurements that rely on sandwich DNA hybridization for capturing a secondary oligonucleotide bearing CdS-nanocrystal tags [36].

1.1.4. Nanopore-Membrane-Based Detection Systems

Nanometer diameter pores have shown great potential for molecular detection and offer some great advantages such as high flow rates, less sample loss, narrow pore size distributions, and they are virtually transparent when wet, making them well-suited for inspection under a bottom-lit microscope. In 2003, Heng, *et al.* showed detection of DNA using silica nanopores [37]. In this work, they had developed CMOS compatible membranes using a high-energy electron beam and, using ionic conductivity measurements, they successfully demonstrated DNA detection. This was the first recorded use of an inorganic membrane for the purpose of discriminating DNA. In another study, modified nanoporous alumina has been used to detect the target DNA by monitoring the increase in the impedance at the electrode [38]. This group modified the membrane with covalently-linked single-strand DNA, which was then used for electrical detection of complementary target DNA sequences. Wanunu, *et al.* [39] have also shown detection of DNA-binding molecules using nanopores fabricated in ultrathin silicon membranes.

1.2. Motivation

With the rapid growth in the area of DNA diagnostics, there is an urgent need for developing a μTAS which can carry out all three of the main tasks involved in DNA diagnostics, i.e. sample preparation or extraction of the DNA, detection, and quantification on a SINGLE chip. Combining these three processes would result in

reduced specimen size, higher yield in extracted DNA, low cost, and affordable disposability with low environmental impact.

Nanoporous aluminum oxide membranes have already shown great potential in the biological and medical fields. Having already presented a successful demonstration of DNA extraction from lysed whole blood using these membranes, our research group, in this particular thesis, is presenting a microfluidics-based, label-free, and electrochemical DNA detection and quantification system based on aluminum oxide membranes. The use of electrochemical detection used in this system promises high sensitivity and selectivity, low cost, inherent miniaturization, portability and no use of classic photolithography techniques.

1.3. Outlines

The growth and development in the field of μTAS and microfluidics has been presented in this chapter. It also discussed some of the state-of-the-art detection systems already developed by various research groups based on different detection concepts. The theory behind electrochemical detection and the importance of nanoporous aluminum oxide membranes will be discussed in Chapter 2. The basic equations used to describe the theory are taken from the previous literature. Design and fabrication of the DNA detection and quantification system will be explained in Chapter 3. The fabrication results and images of the fabricated system will be provided. This chapter will also contain the experimental methods for the quantification of gDNA based on an electrochemical detection concept. Chapter 4 contains the results of the optimization of the detection system. Key parameters, such as the effect of a change in the gap size

between the electrodes, concentration of the DNA, effect of the voltage and the flow rate will also be investigated in that chapter. The last chapter will draw conclusions and summarize the experimental results in this thesis, and it will close with suggestions for future work in this area.

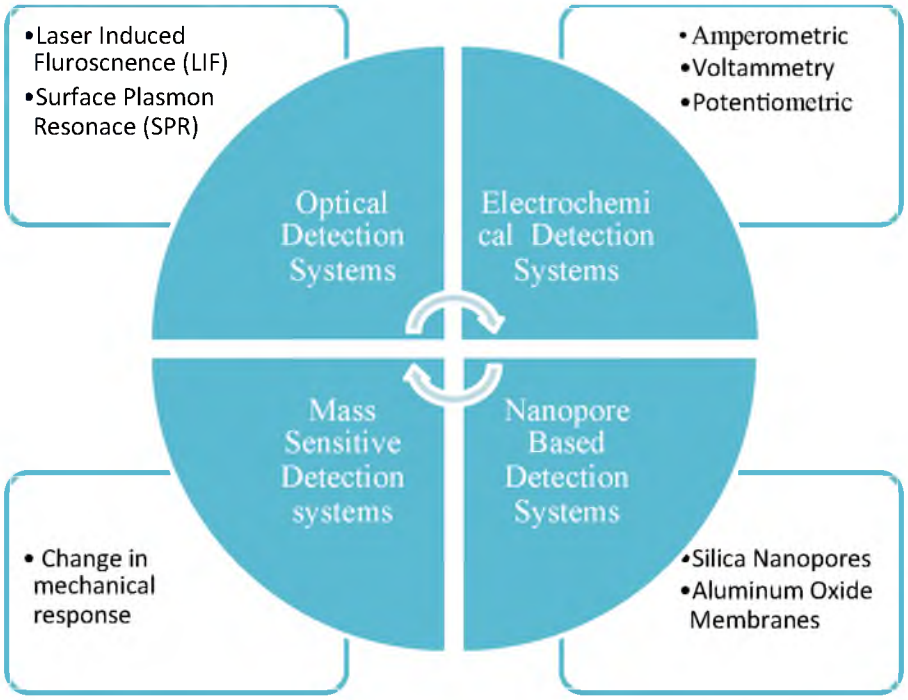

Figure 1.1. Microchip-based DNA detection systems.

CHAPTER 2

THEORY

This chapter focuses on the theory behind the electrochemical detection of different particles at the micro-scale level followed by a description of various properties related to nanoporous aluminum oxide membranes. The theory related to the AOMs will help us better understand their interaction with DNA, so as to enable us to design our DNA quantification system.

2.1. Electrochemical Detection

This section describes the basic theory behind the electrochemical processes that occur during the detection of any particular sample. The electrochemical process is characterized by the transfer of electrons between the electrodes and molecules in the solution in proximity to the electrodes [40]. The fundamental reaction governing the science of electrochemistry is the equilibrium between two species, an oxidizing agent (Ox) that accepts electrons and a reducing agent (Red) that furnishes electrons, represented by the expression:

$$\mathrm{Ox} + e^{-} \rightleftharpoons \mathrm{Red}. \tag{2.1}$$

During the detection of any nanoparticles or biomolecules such as DNA, it is usually assumed that the impedance of the sample to be detected is slightly different from the impedance of the buffer solution carrying this particular sample [41]. When a

constant voltage is applied across the electrodes, it results in an electrochemical reaction causing electrochemically active molecules to be oxidized or reduced, which further results in a gradual change in the rate of transfer of electrons from one electrode to the other, thereby exhibiting a measurable variation in current flow through the circuit [42]. This change in the current can be measured either by measuring the current directly with an ammeter or a voltage drop across a series resistor.

Under ideal equilibrium conditions, electrochemical reactions are governed by the Nernst equation, which is used to determine the equilibrium reduction potential as

$$E = E^0 + \frac{RT}{nF} \ln\left(\frac{C_O}{C_R}\right), \tag{2.2}$$

where, E^0 is the standard potential for the redox couple, T is the Kelvin temperature, n is the number of electrons transferred in the reaction, F is the Faraday constant (96,485 Coulombs), R is the universal gas constant (8.314 J/K·mol), C_O is the molar concentration of the oxidized half of the couple and C_R is the molar concentration of the reduced half.

During the detection of the sample, change in the current (or impedance) in the detection area is possible because of three main reasons. These include:

1. If the sample being detected is electrically conductive, then an increase in current will be observed.
2. If the impedance of the sample being detected is more than the impedance of the bulk solution, then its presence will be signaled by a decrease in the current observed.

3. Interference with the ionic double layer formed at the electrode surface due to the constant potential applied may also result in a change in impedance. This double layer forms at the interface between the electrode surface and the solution, reducing the current in the circuit substantially. Ions in the bulk solution of opposite polarity tend to collect near the surface of the electrode and oppose the voltage, which is created at the electrodes. Thus, a positively charged electrode will have a cloud of negative ions surrounding it, while the oppositely charged electrode would get surrounded by positive ions, causing the effective voltage across the channel to drop. The thickness of this double layer is dependent on two important parameters:
    - Ionic strength of the buffer. Thickness of the double layer increases with the increase in ionic buffer.
    - Flow rate of the buffer. Fast flow rates can help reduce buildup of the double layer.

A disturbance in the double layer will result in an increase of current and once the disturbance is eliminated, the current will drop again and the steady state will be reestablished. This concept of a double layer and the process of diffusion for mass transport making electrochemical detection possible is shown in Figure 2.1.

As summarized in Figure 2.1, an electrochemical reaction is comprised of many different processes that take place during the electrochemical process. When voltage is applied, the oxidized species in the bulk (O*) diffuses towards the electrode resulting in the transfer of its positive charge to form a reduced species (R). This reduced species

with concentration C_R diffuses away from the electrode and back into the bulk solution. During this movement, the distance travelled by the redox molecule by diffusion can determined from Fick's law:

$$x = 2\sqrt{Dt}, \tag{2.3}$$

where, x is the thickness of the double layer, D is the diffusion coefficient of the redox molecule and t is the time taken for the average molecule to travel.

2.2. Electrode Materials

During the electrochemical detection of DNA, the choice of the electrode material carries great importance. Various research groups have successfully demonstrated electrochemical activity of DNA using different electrode surfaces. Palecek studied the electrochemical behavior of DNA near mercury and mercury-amalgam electrodes [43] and showed that mercury electrodes can provide remarkable sensitivity for small changes in the DNA structure. With advantages like wide potential ranges, low electrical resistance, high resistance to corrosion and relatively low cost, carbon materials such as glassy carbon, carbon paste, carbon nanotubes, and graphite electrodes have been widely used for the electrochemical detection of DNA [44]. Gold electrodes have also been used for nucleic acid research, as they offer large double layer capacitance [45] and can be easily patterned with different gap sizes. Various other metals and metal oxides such as indium tin oxide, platinum, and silver have also been used in this area. Table 2.1 provides cited references to some of the studies done by different research groups with various electrode materials for electrochemical detection of DNA.

2.3. Anodized Aluminum Nanoporous Membranes

As the field of nanotechnology continues to grow rapidly, researchers in this field are able to characterize chemical, mechanical, and electrical properties down to the molecular level [46]. Applications of nanotechnology are versatile and one very relevant example of this field is the technology based on synthetic nanoporous membranes. These nanostructured materials have been used widely in different areas such as substrates for biological sensors [47], nano-filtration [48] , DNA extraction system [49] [50] as templates for material engineering [51] [52], separation and extraction of metals [53] [54] and detection of single molecules such as DNA [55] [56] .

Synthetic nanoporous membranes can be divided into three different groups: isotropic (organic and inorganic), track-etch, and nanoporous anodic alumina membranes. The main objective of this thesis is to use anodized aluminum nanoporous membranes or aluminum oxide membranes (AOM) as substrates for extraction, detection and quantification of genomic DNA. The following section will describe the manufacturing process of AOM and their advantages and limitations.

Nanoporous anodic alumina membranes were first reported in the year 1974 when the first patent on electrochemical reduction of aluminum was released [57] and since then, there has been a huge growth in the production of these membranes. Today, these membranes are commercially available from different companies with high open porosity, different pore diameters, and thickness. The pore aspect ratio (pore diameter vs. pore length) can reach up to values of 1:1000 and more [58]. During the anodization process of aluminum, two types of aluminum oxides can be produced on the surface [59]. If the process of anodization is carried out at a pH greater than 5, insulating films will be

formed. However, if anodization is done in strong acidic electrolytes, then a film with pores open to the surface is formed which is known as 'anodized aluminum membranes'. For the fabrication of these membranes, an aluminum foil with purity greater than 99.99 % is desired, which is annealed at 400°C for at least one hour, followed by electropolishing, commonly in a perchloric acid and ethanol solution. After this, anodization of the polished aluminum foil is done in a dilute acidic electrolyte (phosphoric, oxalic, or sulfuric acid) at a temperature below ~10°C. Once the anodization process is complete, then, using a galvanic process, the nonanodized aluminum is removed, and finally the closed ends of pores are opened using dilute phosphoric acid [60] [61] .

The pore diameter is dependent on two very important parameters: applied voltage and time for the anodizing step. High anodizing voltage results in larger pore diameters and can be varied between 1nm to 450nm with a narrow size distribution, a longer anodizing step will give more ordered pores and a large, thick alumina membrane. Asymmetric pores, i.e., pores with different diameters can also be manufactured using two methods. The first method is to vary the voltage during the anodization step and the other method is to change the electrolyte solution during the growth process.

Recently, nanoporous aluminum oxide membranes have shown great potential in the field of genomic diagnostics, particularly in the area of DNA analysis. Many research groups have demonstrated extraction and detection of DNA from lysed human blood using AOMs. Some of the advantages and limitations of these oxide membranes are listed in Table 2.2.

Conventional methods for DNA extraction systems are time consuming and complex and the DNA yield is very low, demanding large and expensive automated systems for sample preparation [62], [63]. Recently, our research group has shown successful demonstration of DNA extraction using a patterned aluminum oxide membrane [12]. In this particular work, we used commercially available AOMs, available from Whatman, Inc., UK, in three different pore sizes, 20nm, 100nm and 200nm.

All three pore sizes and three salt concentrations were tried to find an optimal physical and chemical condition for DNA extraction. The gDNA samples were prepared in salt concentrations of 0M, 100mM, 300mM and 500mM NaCl and the amount of gDNA in the waste solution was measured using spectrometry, determining the amount of gDNA left on the membrane. With no salt concentration, membranes with a pore size of 20nm showed the maximum amount of DNA capture, compared to membranes with 100nm and 200nm pore sizes. However, with an increase in salt concentration, the collection rate for 200nm sized pores increased slowly, so for salt concentrations more than 0.1M, 100% of gDNA was collected over 100nm and 20nm pore sized membranes, making 100nm pore sized membranes the best choice for the extraction process. The improvement in accretion of gDNA on the membrane with increased salt concentration is explained in section 2.4, which mainly discusses the interaction of DNA with aluminum oxide membranes.

2.4. Interaction of DNA with AOM

As discussed above, the pore size of an AOM is one of the most important parameters to be considered during the extraction and quantification of DNA. The

collection rate of DNA for a given pore size is dependent on the pore shape and the aggregation of DNA. When analyte such as DNA binds with the walls of AOM, it has been observed that there are electrostatic interactions between gDNA and the alumina structure, which has many hydroxyl groups on its surface (Figure 2.2). DNA binding to the surface changes the surface charge, which further results in a change of the ionic concentration and conductance through the nanochannel.

When the electrically-charged DNA molecule binds to the surface of the membrane, this ionic resistance will decrease. If the concentration of the salts in the DNA increases, then the normally negatively charged phosphate group of the DNA helix in the solution will get neutralized and the overall charge of the DNA will become neutral and will cause DNA to aggregate.

This chapter has discussed the important theory related to electrochemical detection, different properties of aluminum oxide membranes and the interaction of these membranes with DNA. The chapter also describes the effect of the different pore sizes of AOMs on the yield of extracted DNA. All the important parameters, such as electrode gap size, electrode material, pore size of the AOM and salt concentration are taken into account and have been discussed further in detail in the Chapter 3, which focuses on the design and fabrication of the system.

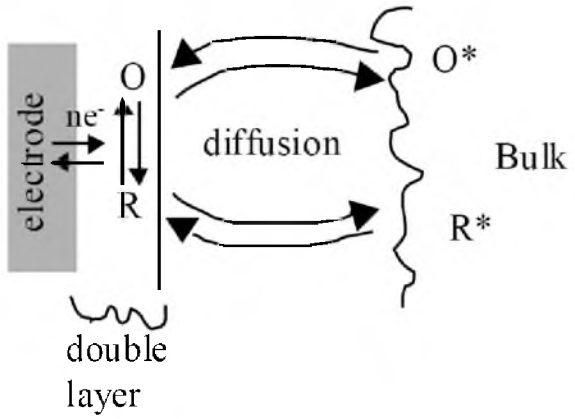

Figure 2.1. Oxidation-reduction process during electrochemical detection.

Table 2.1. Cited references for DNA electrochemical systems with different electrode materials

Electrode Materials	Cited References
Gold	**[64] [65] [66] [67]**
Platinum	**[68] [69]**
Carbon	**[70] [71] [72]**
Mercury	**[73] [74] [75]**
Indium tin oxide	**[76] [77]**
Silver	**[78] [79]**

Table 2.2. Advantages and limitations of nanoporous aluminum oxide membranes.

Properties	Advantages	Limitations
Mechanical	High pore density and narrow pore size distribution. Stability under high pressure. No creeps.	Very brittle, thus difficult to integrate with microfluidics systems. Special needs of configuration or support media.
Chemical	Wide solvent compatibility. Easy electrochemical activity.	
Biological	Extremely low protein binding minimizes sample loss. No sample contamination. Virtually transparent when wet, making it ideal for study under a microscope	
Thermal	Upper operating temperature up to 1100^0C	Sealing is not easy at high temperatures

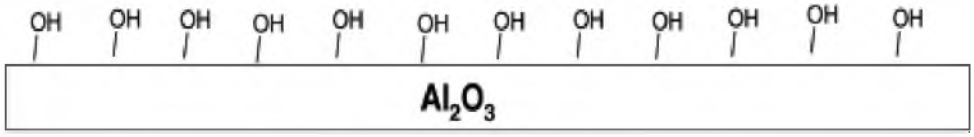

Figure 2.2. Hydroxyl groups attached to the surface of AOM.

CHAPTER 3

DESIGN AND FABRICATION

The following chapter focuses on the methods and techniques for design and fabrication of the integrated DNA extraction and quantification system. A detailed fabrication methodology is presented in section 3.1, which encompasses the step-by-step procedure involved in fabrication of the system. In section 3.1.5 and 3.1.6, both fluidic and electrical connections are discussed in detail along with the problems encountered in patterning and bonding the aluminum nanoporous membrane to PDMS (Polydimethylsiloxane). Lastly, the experimental setup is described in section 3.2, which also discusses the preparation of DNA samples, along with other key parameters.

For the analysis of biomolecules such as DNA, RNA, etc., there is a growing need for shifting all the key processes from classical photolithography methods to some other alternatives. During the detection and extraction of DNA, there is a need for an effective system, which is small in size, portable, inexpensive (so as to be affordably disposable), less dead volume, lower in detection limits, and high yield with regard to the extracted DNA sample. In this thesis, we present an integrated DNA extraction and quantification system that offers all the above listed advantages without use of photolithography. The following part of this chapter focuses on the detailed design and fabrication of this system.

3.1. Fabrication

3.1.1. Substrate

Both borosilicate glass slides and completely etched printed circuit board (PCB), a double-sided copperclad fiberglass board, were used in this work. Two important things were considered during the selection of the substrate material, which are as follows.

3.1.1.1. Strength and Stability

During the fabrication of this device, a substrate was needed that could serve as a platform to which we could easily bond our AOM. There was no concern about the electrical or thermal properties of the substrate, though there was concern regarding the mechanical stability the substrate would provide under normal operation. For these reasons, PCBs and borosilicate glass slides were chosen with thickness of 1.77mm and 1mm, respectively. Before we bond the AOMs to these substrates, we need to provide an outlet for the waste flow leaving the AOMs. For this, a 3mm diameter was drilled with a laser-sighted drill press (GMC) through the PCB, and with a Dremel moto-tool and a diamond bit through the glass slide. Since the drilling of the hole in the PCB is more of a cinch and less time consuming, as opposed to cutting through glass, PCBs were chosen as the main substrate building-block material for most of our experiments. For fabrication of miniature devices, these PCBs were cut into small pieces with dimensions of 30×20mm using a band saw. Once the PCBs of desired dimensions with the drilled holes were ready as shown in Figure 3.1 (step 1), the copper-cladding was completely etched off of these boards on both sides by full immersion in a ferric chloride bath for 20 minutes.

3.1.1.2. Bonding Capabilities and Cost

The next main factors considered in the selection of the substrate material concerned the bonding capabilities with the nanoporous membranes and the cost of these chips. As discussed earlier, for an effective integrated DNA analysis system, it is very important to have a system that is cheap, portable and simple in terms of design and fabrication, and thus, can be used as disposable chips. Based on these factors, fiberglass boards and glass slides were selected for our substrate materials, which both made manufacturing affordable in the quantities needed as well as provided a solid platform for our experimental devices.

3.1.2. Patterning of Aluminum Nanoporous Membranes

Commercially available AOMs, distributed by Whatman, Inc., UK, were used as the filter material for extraction and quantification of gDNA. The precise non-deformable honeycomb pore structure and narrow pore size of these membranes provides high flow rates and less dead volume for our samples. These membranes are available in three nominal pore sizes of 20nm, 100nm, and 200nm, and three diameters: 13mm, 25mm, and 47mm. Earlier, in Chapter 2, we described the effect of different pore sizes on the yield of the extracted DNA and from those results it has been shown that the 100nm pore size maximizes the DNA extraction rate. As, in this work, an integrated DNA analysis system that can simultaneously do extraction and quantification is being fabricated, all the results were characterized with this 100nm pore size membrane. However, results were also obtained with the 200nm pore membranes, as described in Chapter 4, to see the effect of pore size on quantifying DNA during the electrochemical detection.

The primary challenge in working with these membranes was their handling during the patterning, metal deposition, bonding to the substrate and incorporation of these membranes with the microfluidic system. The thickness of these membranes is close to 60µm and they are so brittle and weak in nature, that they get easily damaged during fabrication of the system. To overcome this challenge, these membranes were handled with great care and a new method was developed for their patterning and integration within the microfluidic system. Contact of these membranes with monomers, adhesives, surfactants, or wetting agents was avoided during the fabrication process, to ensure they remained ultra-pure without necessitating their cleaning at any stage.

During the pattering of these membranes, the fabrication of the channel on this membrane was the first most important part of the whole system, as it not only acts as the insulating spacer between the two electrodes but also defines the extraction and quantification area. Using a knife plotter (FC5100A-75, Graphtec Inc.), a shadow mask with straight channels was cut on a Rubylith film, which consists of a UV opaque red emulsion on clear polyester backing without an adhesive. To see the effect of various geometrical dimensions on these systems, we cut the film three different ways, with widths of 50µm, 100µm, and 200µm, and attached these to different membranes electrostatically.

3.1.3. Electrode Materials

Once each membrane with the shadow mask was ready, the electrodes were fabricated on the membrane itself. These electrodes are required to be highly planar and conductive. Sputtering (TMV sputtering systems) was used to deposit gold metal on the

membranes. Since, these membranes are so brittle and thin, they cannot be loaded directly in the sputtering chamber, as it will damage the membranes. For this reason, the patterned AOMs were taped to a glass slide that served as a platform during the metal deposition process. Gold metal was deposited at 90W with a process pressure of 10mT for 10 minutes, which produced a layer with a thickness of 250nm. After the metal deposition was completed, the membranes were carefully removed from the glass slides and the shadow masks were equally carefully peeled off from the membranes with tweezers. These AOMs with a narrow channel between the electrodes were inspected under an SEM (scanning electron microscope) to measure the channel width and to see the pores between the electrodes (Figure 3.2).

3.1.4. Membrane Bonding to the Substrate

Another challenge in the fabrication of the system was bonding of thin patterned membranes to the PCB or glass substrate. For this process an adhesive (Loctite 4011) was applied in small dots using a syringe needle behind the patterned membrane and afterwards this membrane was aligned with the PCB substrate in such a way that the channel between the electrodes on the membrane aligned with the center of the drilled hole on the PCB. Care was taken not to apply substantial pressure during the bonding, as it could easily break the membrane.

Once the channel was perfectly aligned and bonded with the hole on the PCB as shown in the fabrication flowchart (Figure 3.1, step 2), the system was kept in a clean box to avoid contamination of the channel from dust particles.

3.1.5. Inlet and Outlet Ports

An important and crucial part of this system was integration of the patterned membranes with the microfluidics to fabricate inlet and outlet ports. This was achieved by attaching aluminum membranes with a PDMS tape that was further bonded to a thick PDMS slab. Fabrication of the PDMS tape was accomplished by taking a double-sided tape (Scotch tape 3M 2000MP), which was peeled from the four sides and bonded over a Petri dish. Liquid PDMS (Dow Corning Sylgard 184 Silicon Elastomer Base) was mixed for 2 minutes with a cross-linking agent (Dow Corning Sylgard 184 Silicone Elastomer Curing Agent) at a volumetric ratio of 10:1 and then the mixture was placed in a vacuum chamber for approximately 40 minutes to remove all the air bubbles from the PDMS mixture. The petri dish with the double-sided tape was loaded over the spinner (Laurell technologies Model: WS-400A-6NPP/LITE) and 10mL of a bubble-free PDMS mixture was poured over the double-sided tape, and the spinner was spun for 30 seconds at 1500rpm to get a thin layer of PDMS over the double sided tape. After the process was complete, the petri dish was placed in an oven at 65°C for 70 minutes to cure the PDMS. To make a PDMS slab with a thickness of 3mm, 30mL of bubble-free PDMS was poured into another small petri dish and placed in the oven at the same temperature and for the same time.

Once the PDMS/tape composite and the thick PDMS slab were completely cured, they were removed from the petri dish and were cut into small blocks with dimensions of 5mm×5mm using a sharp steel blade. To connect the surface of the membrane with the tubing through these PDMS layers, a 2mm diameter hole was cut in the PDMS tape as well as the thick PDMS slab, separately, using a coring tool. Corona discharge (Enercon

Dyne-A-mite 3D Treater) with an output voltage of 15kV was used for bonding of PDMS tape to the thick PDMS slab. Both surfaces were exposed for 40 seconds to the corona discharge and the cored holes on the PDMS tape and the slab were aligned properly under the microscope, after which the complete block was baked in a 65°C oven for 40 minutes

Once cured, the backing tape was removed from the PDMS tape using a pair of fine tweezers and the adhesive side of the complete PDMS block was bonded over the patterned membrane under the microscope in such a way as to allow the inlet port in the PDMS block to align accurately with the channel on the membrane. To make the outlet port, an identical block of PDMS tape and with a thick PDMS slab having a cored hole of same diameter was fabricated and attached to the bottom side of the drilled hole on the PCB substrate. Care was taken to align the inlet and outlet ports with each other using alignment marks. Finally, the integrated system was placed in a 65°C oven for 30 minutes, so as to increase the bond strength (Figure 3.1, step 3).

3.1.6. Electrical Connections to the System

After the integration of inlet and outlet ports with the patterned membrane, the next key step includes producing electrical connections to the system. The electrical connections were created by bonding thin wires with both electrodes on the membrane, using a two component conductive silver epoxy (MG chemicals). Further, to cure the epoxy, the system was placed on a 150°C hot plate for 15 minutes (Figure 3.1, step 4). Figure 3.1, step 5 shows the complete fabricated DNA extraction and quantification device with electrical and fluidic connections.

3.2. Experimental Setup

The experimental setup for the integrated DNA detector system characterization consists of two syringe pumps, sample injection units and a pressure gauge in addition to the just-fabricated integrated microsystem device. The required DC supply to the detector system was provided by a source meter (Keithley 2400), which was also able to measure current and resistance. The source meter was connected to the PC through a GPIB card, and data was collected and then analyzed using LABVIEW software (version 8.5). The reason for choosing a syringe pump (model 100, K-D Scientific) instead of a peristaltic pump is due to the requirement of a constant flow rate. All fluidic tubing and connectors were obtained from Upchurch Scientific. The experimental flow chart for the system is schematically shown in Figure 3.3 and the experimental set up is shown in Figure 3.4.

A 3mL and 1mL Becton-Dickinson plastic syringe was used to pass the buffer solution and gDNA of different concentrations. The detector system was characterized on the basis of three key parameters: concentration of the gDNA, applied voltage, and corresponding current and the channel size between the electrodes. In order to know the detection limit and sensitivity of the system, the detector system was tested with different concentrations of gDNA. The initial concentration of gDNA sample was 54ng/μL, which was further diluted to 27ng/μL, 13.5ng/μL, 10.1ng/μL, 6.75ng/μL and 3.2ng/μL by addition of equal amounts of Tris EDTA (TE) buffer and 1% Triton X-100 solution. Triton X-100 agent in the buffer solution acts as a non-ionic surfactant, which simplifies membrane dewetting and decreases flow resistance that serves our purpose of decreasing the entire process time. Total sample volume was 400μL, which includes 200μL of gDNA sample with a known concentration, 100μL of TE buffer and 100μL of 1% Triton

X-100 solution. 100μL of this sample solution was passed through the detector system with a 7μL/min constant flow rate from the syringe pump at room temperature.

Voltages applied to the electrodes in the detector system ranged between 2V and 4V. As mentioned earlier, the nanoporous membranes were patterned with three different channel sizes between the electrodes. The widths of these channels on the membrane were 50μm, 100μm and 200μm. For all these experiments, along with the requirement of a stable current, the voltage supply was provided following the injecting of the sample into the detector using a syringe. Constant attention was paid to ensure there were no leaks in any of the experiments, to the integrity of the electrical connections and the bonding of nanoporous membrane with the PDMS tape and slab.

In this chapter, a detailed description of the fabrication of the integrated DNA extraction and quantification system using AOMs bonded to PDMS tape was provided. The experimental scheme to test the fabricated system using different concentrations of DNA was described. In the next chapter important parameters associated with DNA quantification systems will be studied and different concentrations of DNA will be quantified.

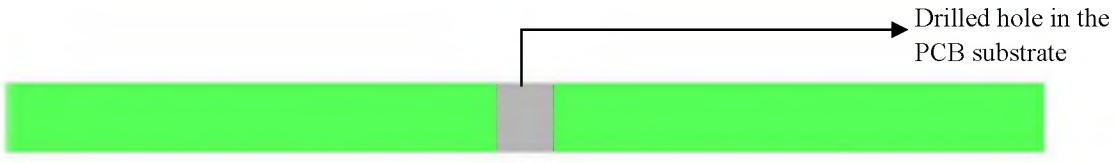

Step 1: PCB substrate with a drilled hole in the middle

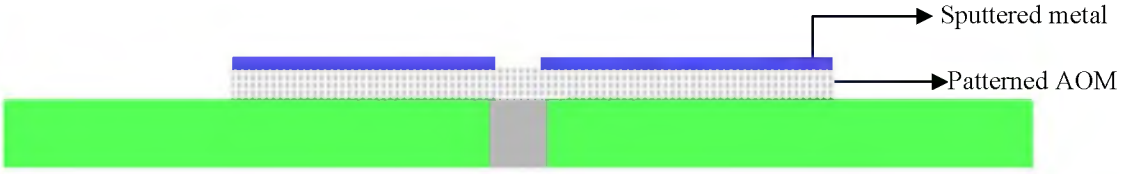

Step 2: Bonding of patterned aluminum oxide membrane to the substrate

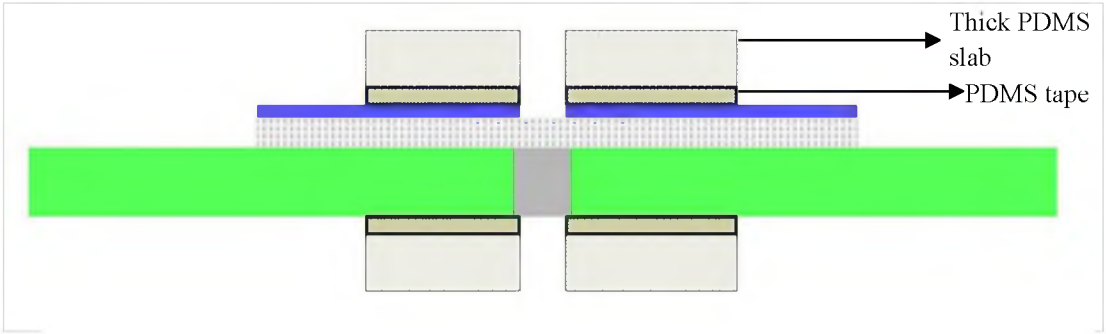

Step 3: Bonding of PDMS tape and slab to the aluminum oxide membrane

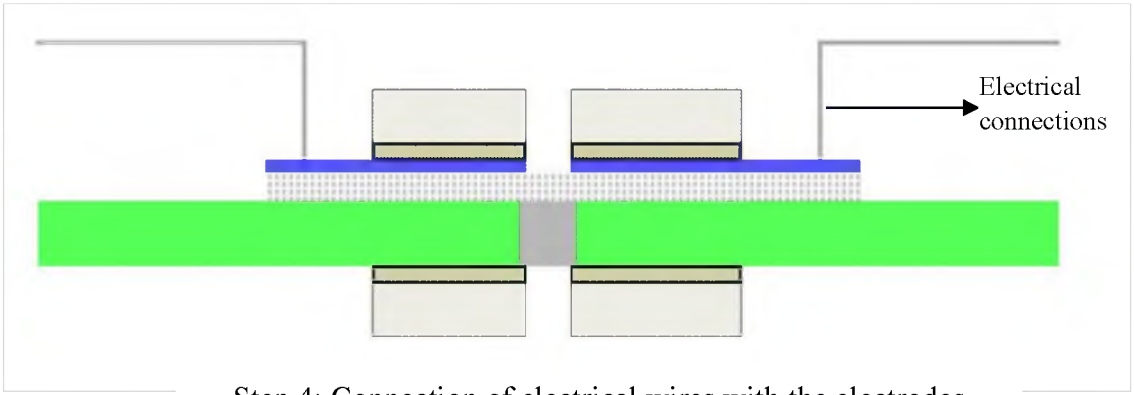

Step 4: Connection of electrical wires with the electrodes

Figure 3.1. Fabrication flow chart for the integrated DNA extraction and quantification system.

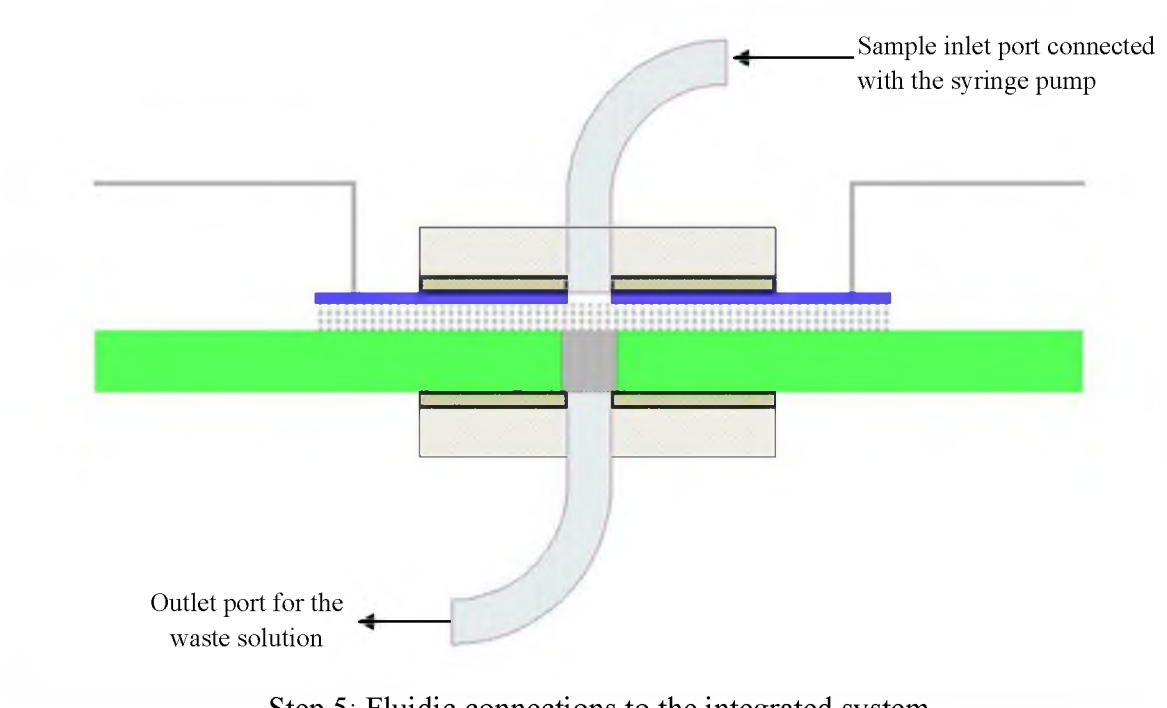

Step 5: Fluidic connections to the integrated system

Figure 3.1. Continued.

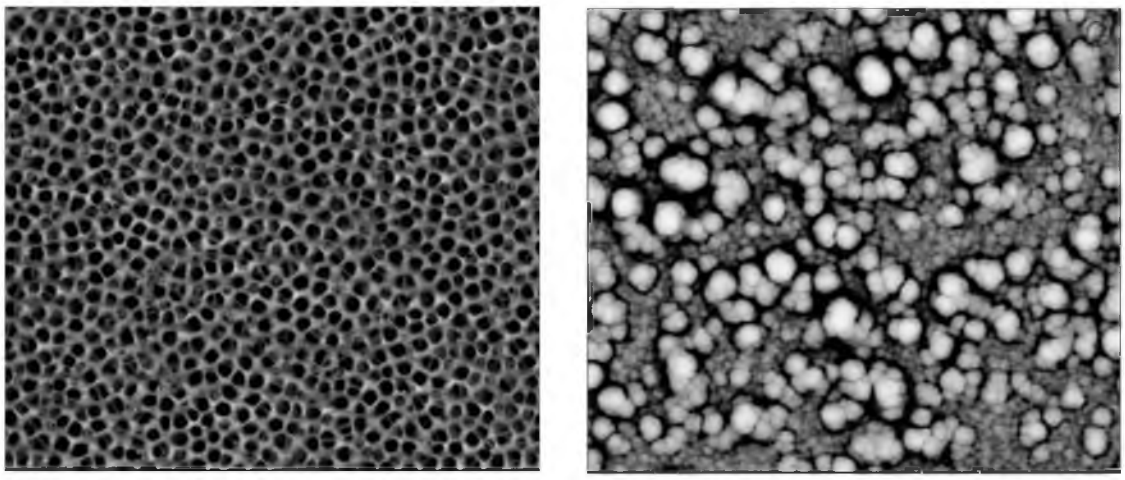

(a) (b)

Figure 3.2. SEM images of the 100nm AOM between the electrodes (scale 4μm) (a) and gold metal deposited on the membrane (scale 2μm) (b).

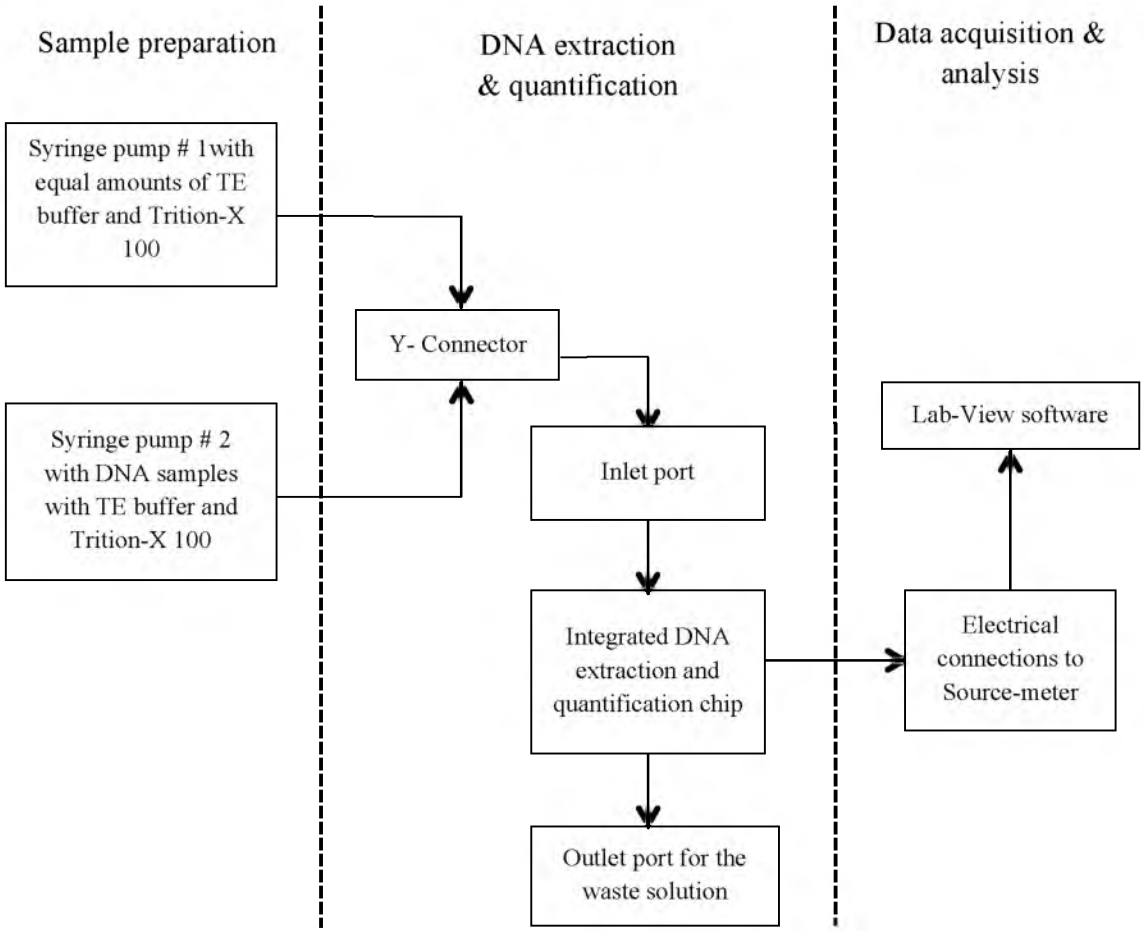

Figure 3.3. Experimental setup flowchart for the integrated DNA extraction and quantification system.

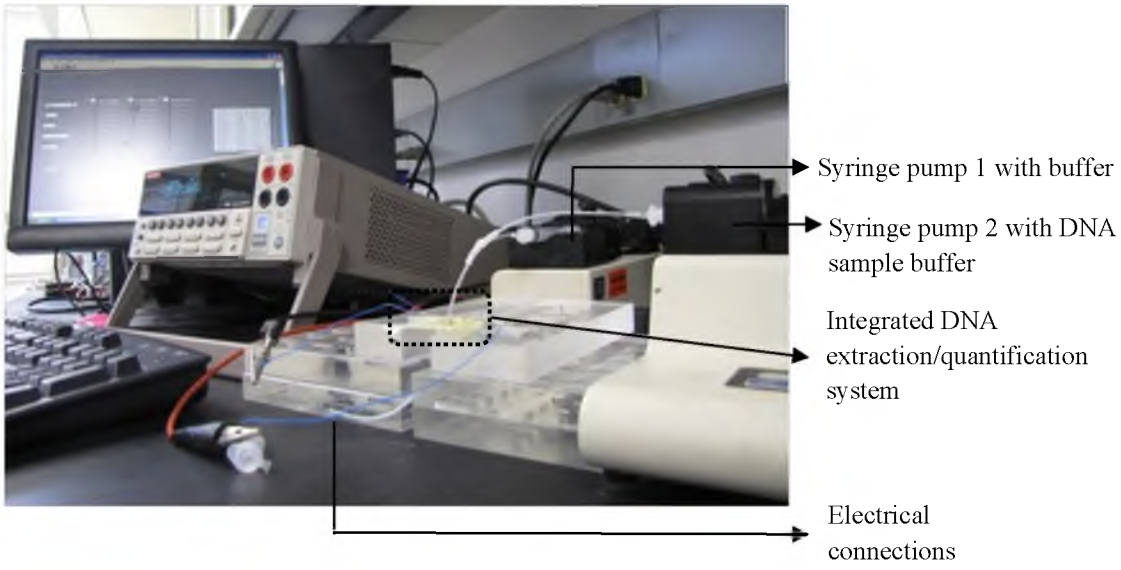

Figure 3.4. Experimental setup for the integrated DNA extraction and quantification system.

CHAPTER 4

RESULTS

This chapter discusses the experimental results obtained for the characterization of the integrated DNA extraction and quantification system. It first elaborates the effects of flow rate, voltage, and channel size between the electrodes on the system followed by the evaluation of the results. The results are based on three different experimental setups which are discussed thoroughly. Finally, the chapter concludes with a detailed discussion on a calibration curve and formula for quantifying any unknown mass or concentration of DNA.

4.1. Experiment I: Experiments with DNA Samples Only

Figure 4.1 shows the cross-section and top view of the fabricated DNA extraction and quantification chip. A large number of these chips were fabricated in identical manner, and a new one was used for each experiment.

As the negatively charged DNA molecules start to bind with the surface of AOMs, they start blocking the pores of these membranes, which results in a large residual extraction of DNA on top of these membranes. During the electrochemical quantification of the DNA, it was anticipated that when gDNA molecules begin to bind with the surface of AOM, the current might increase with the increase in the mass of the DNA extracted over the membrane. At a certain point, when all the pores of the membrane get blocked,

because of the binding of gDNA, the system would reach a constant current, which will be directly related to the maximum mass of the gDNA collected over the membrane. In the first set of experiments when this system was fabricated, gDNA with a specific concentration in the buffer solution was passed directly through the system and the change in the current was measured. For all the set of experiments, three important parameters were considered and studied in detail. These included:

- Voltage: High voltage was not used on this system, as high voltages resulted in extensive bubble formation and electrolysis. At considerably higher voltages, the presence of aqueous carrier leads to the unwanted phenomena of bubble formation, which causes an increase in the signal-to-noise ratio, affecting the sensitivity of the system. Thus, a constant voltage of 2.5V was applied across the electrodes.
- Channel width: The channel size between the electrodes for extraction and quantification of DNA was kept constant at 100μm. With larger channel widths the electrolyte resistance outside the pores was too large, resulting in poorer signal-to-noise ratios. Because we are doing simultaneous extraction of gDNA along with the quantification, smaller channel widths limit the yield of extracted gDNA, and thus were not desirable.
- Flow rate: As per the discussion in the previous chapter, a syringe pump providing a constant flow rate was used to pass all the sample solution into the system. The system was tested with different flow rates to see the effect on the change in the measured current. With higher flow rates (20-30μL/min), the waste buffer solution took more time to drain off the membrane as per the small

extraction area on the membrane, which caused clogging of the buffer resulting in an unstable increase in current. Once having undertaken these observations, the flow rate was decisively decreased and the system responded with more efficient results at 7μL/min.

After the optimization of all the important parameters, 400μL of sample volume, which includes 200μL of gDNA with a concentration of 10.1ng/μL, 100μL of TE buffer and 100μL of 1% Triton X-100 solution, was passed through the quantification system at a constant flow rate of 7μl/min using a syringe pump for approximately 20 minutes.

Figure 4.2 presents a graph showing the measured current (A) as a function of time (s) for DNA concentrations of 10.1ng/μL and 0ng/μL, when a constant voltage of 2.5V was applied across the electrodes. The first 5 minutes were taken to drive the air out of the system until the sample reached the membrane. As the sample touches the surface of the membrane we see a sudden increase in the current, which is just an electrochemical effect and can be ignored. The peak drops exponentially as the double layer is formed. For the sample solution with 0ng/μL of DNA (only TE buffer and Triton-X 100), we notice that the current falls steadily and levels off at 3.12μA. However, for the other sample solution with a DNA concentration of 10.1ng/μL, the current starts increasing linearly from 3.57μA to 15.2μA as the DNA molecules starts binding with the surface of membranes and allowing more current to flow. At this point we noticeably see that after approximately 210 seconds, the current saturates at 15.3μA.

To check the repeatability of the detector response, three separate runs with the same concentration, sample volume and different devices were carried out, resulting in the same increase in current in each case. The graph showing the repeatability of the

results with this experiment is discussed in Appendix A. After completing the first set of experiments, it was not clear if the increase in current was because of the DNA molecules binding with the surface of the membrane or if the increase was due to the salt concentration or any other particles. To validate these results we carried out a second set of experiments, which are discussed in the next section.

4.2. Experiment II: Experiments with Buffer Solution and DNA Samples

In contrast to the initial results that were obtained by just pumping DNA samples directly through the system, our second set of experiments was carried out in two steps. In the first step, only the buffer solution, which was the mixture of TE and Triton-X 100, was allowed to flow through the system for approximately 5-7 minutes, followed by the injection of DNA sample into the system for about 10 minutes. For this particular experiment, two syringe pumps and a T-connector were used. The first syringe pump was used to pump 600μL of buffer solution, which was without any DNA, and the other syringe pump was used to pump 200μL of DNA samples into the system. Both the syringes were connected to the T-connector through the tubing and one end of the T-connector was connected to the system. All the other parameters such as the flow rate, voltage and the channel gap size were left unchanged.

Figure 4.3 shows a graph that presents the measured detector response as a function of time for two concentrations of gDNA, i.e., 0ng/μL, 6.67ng/μL. The first 2 minutes were taken up by the air being driven out of the system. Once the buffer touches the membrane, one notices the electrochemical peak for all the runs which is to be ignored. Once the buffer solution begins to pass smoothly through the aluminum oxide

membrane it is clear that the current levels off at 3.17μA with no DNA present (0ng/μl). In the second case the buffer solution was pumped for 5 minutes and then the DNA sample, with a concentration of 6.67ng/μL, was injected into the buffer solution and passed through the system. For the first 5 minutes, the current remains fairly stable at 3.23μA and as the DNA starts binding with the surface of the aluminum oxide membrane, we notice the linear increase in the current. After approximately 480 seconds, the current appears to saturate at a value of 10.5μA, which suggests that most of the pores are blocked with gDNA. For each concentration of gDNA, three runs with the same sample volume and flow rate were run through distinct but identically fabricated systems. The graph showing the repeatability of the results with this experiment is discussed in Appendix A. In order to validate the results further, we conduct our third and last experiment.

4.3. Experiment III: Experiments with Buffer Solution, DNA Samples and Buffer Solution

In the previous section, we used an experiment in which the buffer solution was pumped through without any DNA for a particular time period and then DNA was injected into that buffer solution. From the graphs, we could deduce that the increase in current did not occur until after the DNA molecules were injected into the solution, presumably due to the higher conductivity of the DNA. In order to further validate these results, a third and last experiment was taken, which we break down into three detailed steps. First step, buffer solution is pumped through at a similar flow rate as previously for about 2-3 minutes followed by step 2, the injection of DNA samples into the buffer

solution for approximately 10 minutes. In the third step, buffer solution is again passed through the membrane without letting any DNA molecules into the system for 2-3 minutes. Now, if there is an increase in the current as a result of any salt concentration or any other particles, then the current should decrease to its saturation limit same as for the results that had been obtained for the buffer solution before. If the current falls to the previous levels before DNA is injected, then it is proven that that there are no DNA molecules trapped on the surface of the membrane. However, if the current still remains at the same level after the pumping of the buffer, then it is established that the pores of the aluminum oxide membrane are blocked with the DNA molecules and the increase in the current is an outcome of the presence of DNA molecules at the surface of the membrane.

Figure 4.4 represents a graph of the result of this planned sequence. It can clearly be seen that in the first step the buffer solution without any DNA gives us the same constant current of 3.23μA as attained through our previous experiments. When the DNA is injected into the system, the current starts to increase and saturates at 10.6μA, giving the same amount of saturation current in approximately the same time as before.

After 10 minutes when the buffer solution without any DNA is injected again, the current decreases from 10.6μA to 9.8μA, but after some time it becomes constant at 9.6μA. Figure 4.5 shows another graph which represents the detector response (A) plotted against time (s) for five different concentrations of gDNA, i.e., 0ng/μL, 3.3ng/μL, 6.7ng/μL, 10.1ng/μL and 13.5ng/μL. For all the concentrations, the same voltage, sample volume, extraction area and time were used.

4.4. Calibration Curve

The main objective of designing and fabricating this system was to extract a certain amount of gDNA on the surface of aluminum oxide membrane and quantify the extracted mass of gDNA. Quantifying the mass or concentration of gDNA can help in determining the amount of sample required during the amplification, which is typically the next step in a genetic analysis system. Quantification of the gDNA will also eliminate many steps required during PCR, thus saving time and resources.

From the experimental results in the previous sections, we can plot a calibration curve through which the concentration of gDNA in any unknown sample can be determined. Once we can quantify the concentration of the gDNA, the mass extracted over the surface of the membrane can be determined using the following equation:

$$m = [c]Qt \tag{4.1}$$

where m is the mass of the gDNA collected over the membrane, $[c]$ is the concentration of the gDNA which can be quantified using the calibration curve, Q is the volumetric flow rate which is constant for these experiments, t is the run time of that concentration through the membrane.

For obtaining the calibration curve, we calculated ΔI_S from the graph presented in Figure 4.5. ΔI_S, which we can say as a detector response, can be determined as:

$$\Delta I_S = I_{S(DNA)} - I_{S(Buffer)} \tag{4.2}$$

where $I_{S(DNA)}$ is the average of the saturation current after injection of the DNA samples into the buffer and $I_{S(Buffer)}$ is the saturation current or the reference current from the buffer solution in the absence of any DNA samples. The detector response was calculated

for three runs each time for a particular concentration of the gDNA and the average of that data was plotted as a function of the concentration of the gDNA and the linear trend line was fitted to that data. Figure 4.6 represents the calibration curve for the quantification of gDNA, which shows the detector response ΔI_S (A) as a function of the concentration of the gDNA (ng/µl).

Error bars with the standard deviations are added to the graph and the trend line has a coefficient of determination, R^2, value of 0.99. The results from the characterization experiments of DNA quantification system were found reasonable. Based on these experimental plots and the calibration curve, the concentration of gDNA and the amount of mass extracted on the surface of the aluminum oxide membrane can be determined within 10 minutes. The minimum concentration of gDNA that was quantified using this system was 3.3ng/µL, and with narrower channel sizes between the electrodes this system could also quantify even lower concentrations of gDNA. The system also showed good results in terms of the bonding of PDMS tape with the aluminum oxide membrane after the extraction of the gDNA. Furthermore, the extracted gDNA can be eluted easily from the surface of membrane using an elution buffer for further analysis.

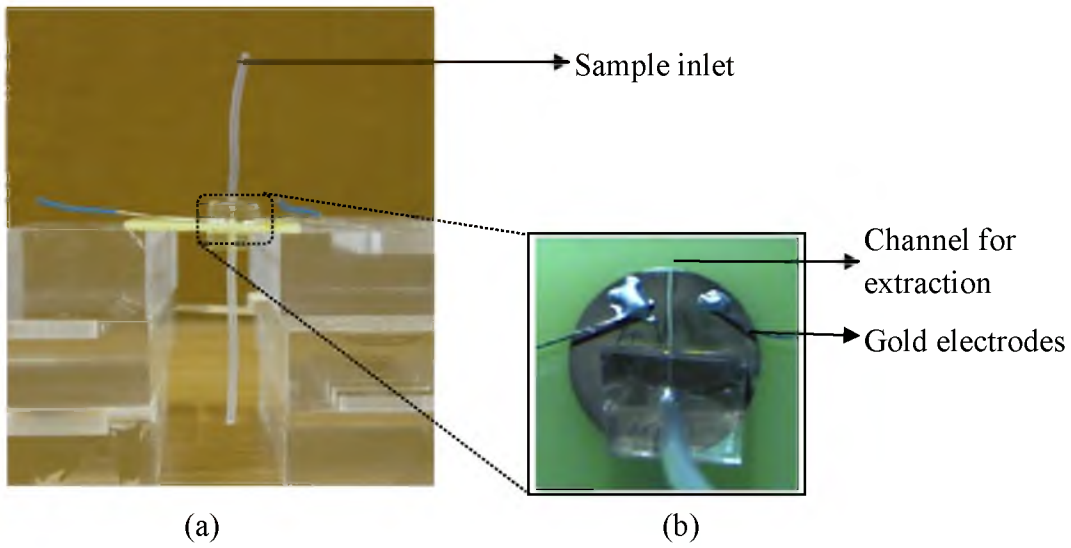

Figure 4.1. Cross-section (a) and top (b) view of the fabricated DNA extraction and quantification chip.

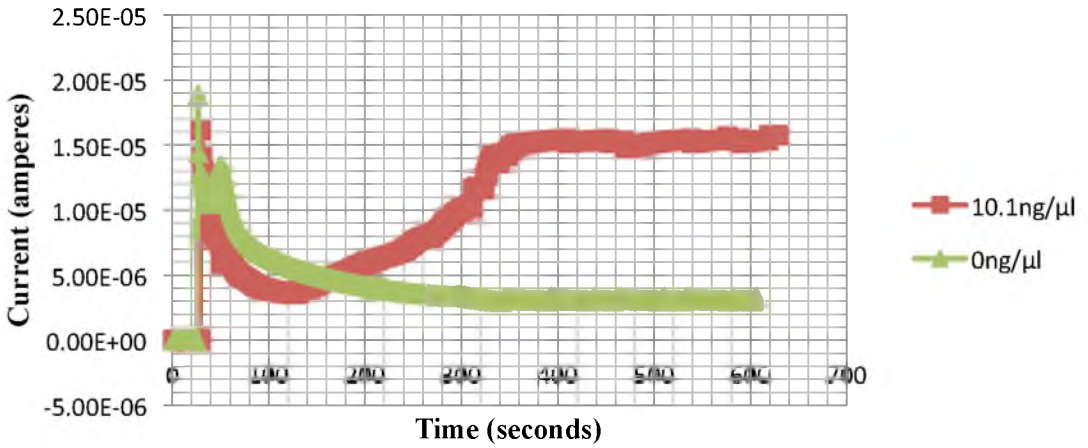

Figure 4.2. Graph with two concentrations of gDNA (0ng/µL and 10.1ng/µL). The system sources a constant saturation current for 0ng/µL, whereas for 10.1ng/µL, current increases linearly till the membrane pores are completely blocked with gDNA and then provides a constant current related to the mass of gDNA deposited on the membrane.

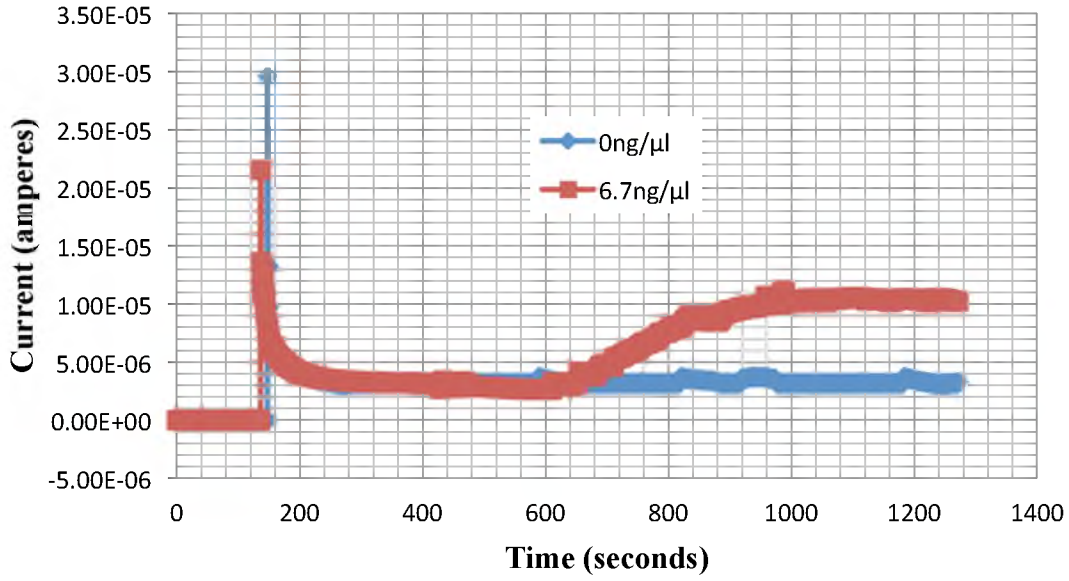

Figure 4.3. Graph with two concentrations of gDNA (0ng/µL and 6.67ng/µL). The system shows a linear increase in the current when DNA starts to bind with the surface of membrane. For 0ng/µL concentration of DNA, no increase in the current can be seen.

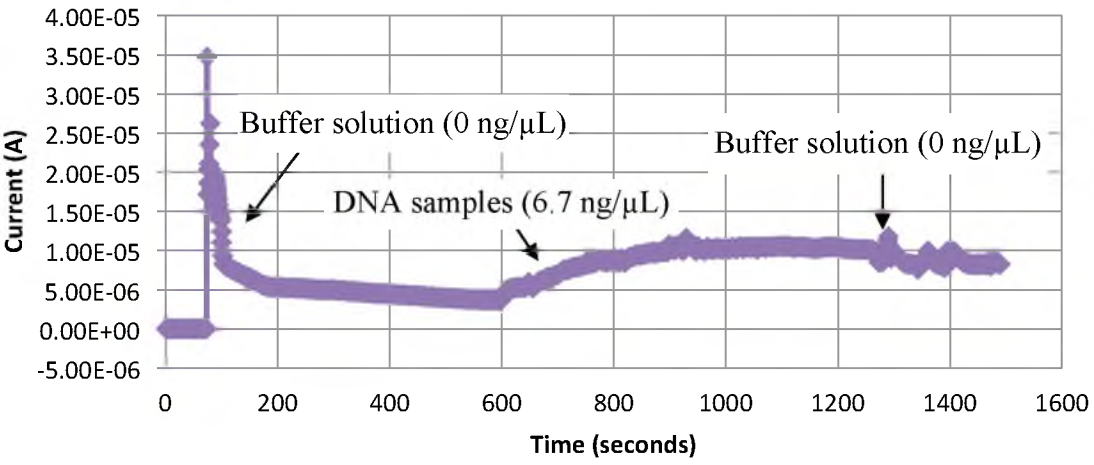

Figure 4.4. Experiment III, with DNA concentration of 6.7ng/µL. For the first 3 minutes only buffer solution (0ng/µL) was pumped through the system, followed by injection of DNA samples for 10-12 minutes into the system. After 10 minutes, buffer solution (0ng/µL) was again pumped through the system.

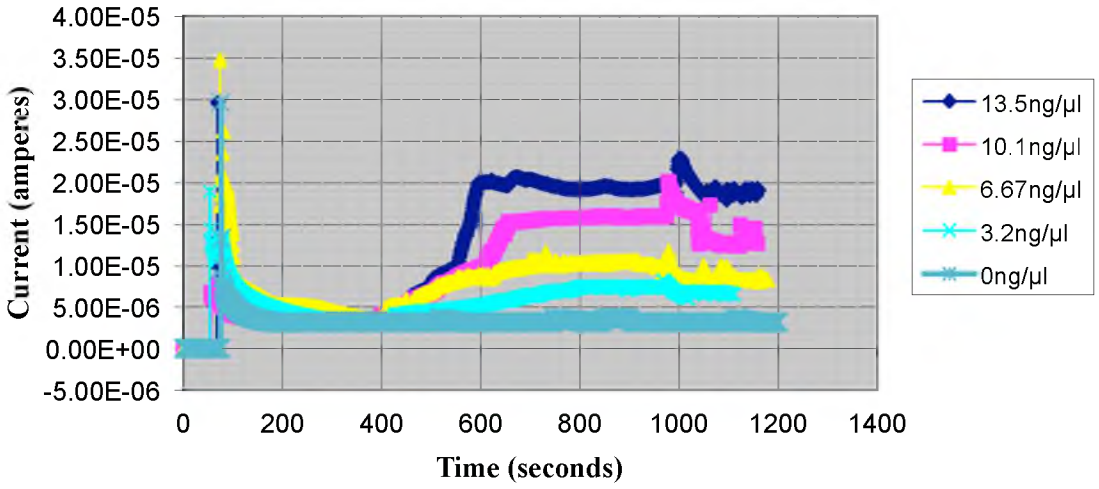

Figure 4.5. A graph showing the change in the current through the system as a function of time for different concentrations of gDNA samples. The current started to increase linearly as soon as DNA samples were injected into the buffer solution.

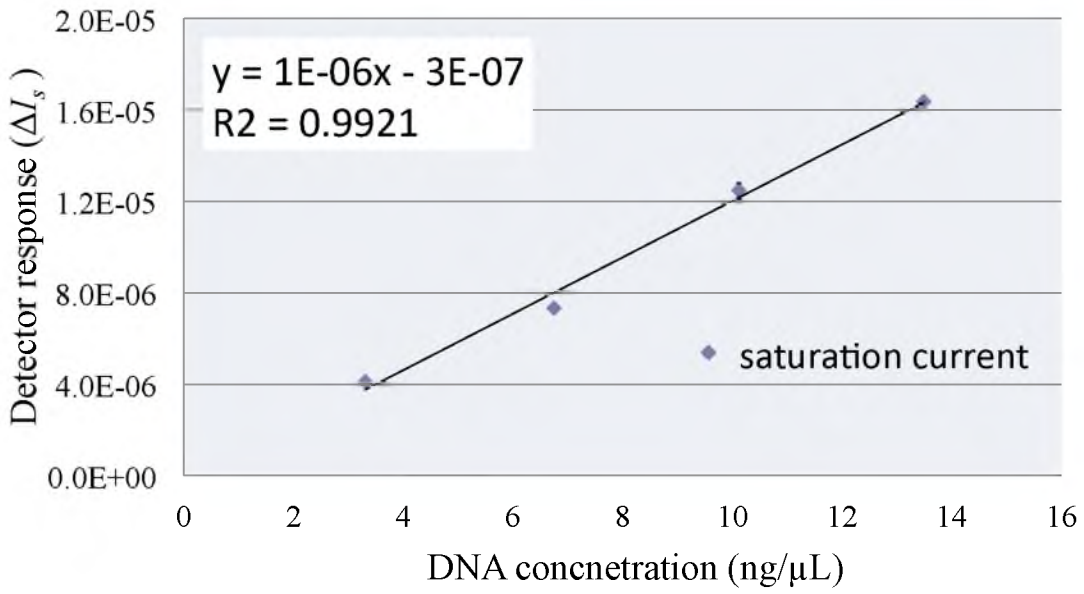

Figure 4.6. Calibration curve representing the empirical relationship between the detector response (ΔI_s) and concentration of gDNA samples. Error bars with the standard deviation are added. The concentration of any unknown sample can be determined using this relationship.

CHAPTER 5

CONCLUSIONS

An integrated DNA extraction and quantification system using aluminum oxide nanoporous membranes (AOM) was designed and fabricated successfully. Initial work related to the detection and quantification of DNA using different concepts has been presented via this work. The theory behind the electrochemical detection was explored thoroughly and also the binding of DNA molecules with the surface of AOMs along with the effect of different pore sizes of nanoporous membranes was studied in detail. The system was fabricated using AOMs as substrates for the extraction of gDNA, bonded with the PDMS block for providing the microfluidic inlet and outlet. The fabrication procedure for this system eliminates the need for the systems based on classical photolithography methods.

Characterization of the DNA extraction and quantification system was derived based on several parameters such as different concentrations of gDNA, voltage applied, flow rate and channel gap size between the electrodes. Three experiments with different experimental setups were applied to see the binding effect of DNA with the surface of AOM. The current was found to be linearly related to the concentration of gDNA. Using the experimental data, a calibration curve was obtained through which concentration and mass of gDNA in any unknown sample can be determined successfully.

This system thus provides us with several advantages such as the simultaneous extraction and quantification of gDNA, low detection limit of DNA (3.3ng/μL), less sample volume (200μl), high sensitivity and selectivity, low cost, small size, fast analysis time (less than 10 minutes), portability and disposable chips and more yield in extracted DNA compared to other quantification systems. Overall, when implemented in the area of DNA analysis this system can prove to be highly functional and valuable.

5.1. Future Work

This thesis work has demonstrated successful fabrication of an integrated system that can extract and quantify gDNA simultaneously from any unknown sample. In the future, the experimentation would move to a higher realm of achievement while quantifying gDNA from blood samples, which will certainly save time and other resources. Other applications of this system include successful integration with a genetic analysis system. With different pore sizes of AOMs connected in series or parallel on one chip, this system can also be used for extracting and quantifying different biomolecules such as RNA, proteins and nanoparticles simultaneously.

Currently, the main problem with this system is the brittleness of the nanoporous oxide membranes. Under high pressures or stretching of electrical wires, these membranes tend to fracture easily and once the membrane is broken, the whole system fails. In this system, the electrical connections are made directly from the membrane to the source meter. As an alternative to these direct connections, one could make electrical connections in two steps. In the first step, a positive photoresist coated PCB board, patterned with bond pads on that PCB could be prepared according to certain

specifications and design. Secondly, after patterning, the membranes are to be bonded on that PCB and using epoxy one can connect the electrodes on the membrane with the bond pads on the PCB that can be further soldered to long electrical wires connected to the source meter. Finally, I would also suggest that integrating this system with pneumatic micro valves would further increase the portability of the system, thus revolutionizing the whole methodology of DNA extraction and quantification.

APPENDIX A

REPEATABILITY GRAPHS WITH DIFFERENT EXPERIMENTS

Figure A.1 presents a graph showing the measured current (A) as a function of time (s) for three runs with three different systems for DNA concentration of 10.1ng/μL following the experiment I, when a constant voltage of 2.5V was applied across the electrodes. For all the three runs, the system showed approximately the same saturation current and, for DNA concentration 0ng/μL, no increase in the current was observed.

Figure A.2 represents a graph showing the measured current as a function of time for three runs with three different systems for DNA concentration of 6.7ng/μL following experiment II, when a constant voltage of 2.5V was applied across the electrodes. For all the three runs, the buffer solution without any DNA samples was passed for the initial 10 minutes followed by injection of DNA samples with the concentration of 6.7ng/μL. All systems showed approximately the same saturation current for DNA concentration of 6.7ng/μL and for DNA concentration 0ng/μL no increase in the current was observed.

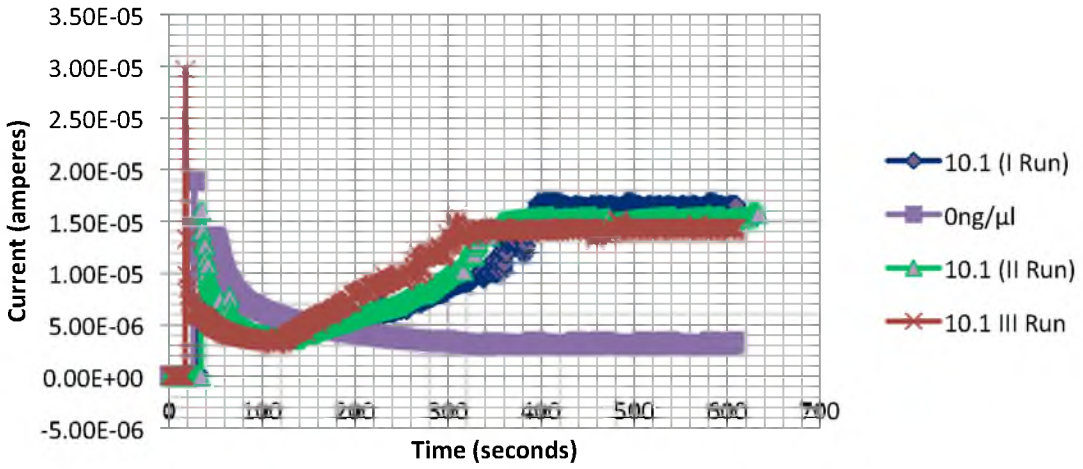

Figure A.1. Graph with experiment I for three runs of same concentration of gDNA (10.1ng/µL) with three systems showing the repeatability of the results.

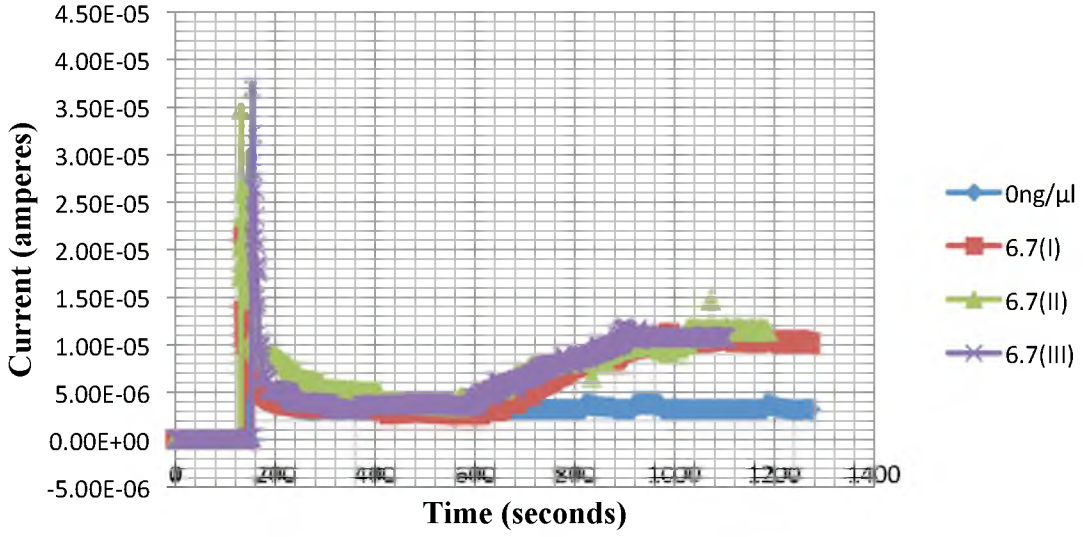

Figure A.2. Graph with experiment II for three runs of same concentration of gDNA (6.7ng/µL) with three systems showing the repeatability of the results.

REFERENCES

[1] A. Manz, N. Graber, and H. Widmer, "Miniaturized total chemical analysis systems: a novel concept for chemical sensing," *Sensors and Actuators B: Chemical,* vol. 1, pp. 244-248, 1990.

[2] D. Frigstad, *Growth Partnership Service: Drug Discovery Technologies*. Available: http://www.frost.com/prod/servlet/svcg.pag/HCDD

[3] T. Vilkner, D. Janasek, and A. Manz, "Micro total analysis systems. Recent developments," *Analytical Chemistry,* vol. 76, pp. 3373-85, Jun 15 2004.

[4] K. A. Wolfe, M. C. Breadmore, J. P. Ferrance, M. E. Power, J. F. Conroy, P. M. Norris, *et al.*, "Toward a microchip-based solid-phase extraction method for isolation of nucleic acids," *Electrophoresis,* vol. 23, pp. 727-733, 2002.

[5] M. G. Elgort, M. G. Herrmann, M. Erali, J. D. Durtschi, K. V. Voelkerding, and R. E. Smith, "Extraction and amplification of genomic DNA from human blood on nanoporous aluminum oxide membranes," *Clinical Chemistry,* vol. 50, pp. 1817-1819, 2004.

[6] T. Nakagawa, R. Hashimoto, K. Maruyama, T. Tanaka, H. Takeyama, and T. Matsunaga, "Capture and release of DNA using aminosilane-modified bacterial magnetic particles for automated detection system of single nucleotide polymorphisms," *Biotechnology and Bioengineering,* vol. 94, pp. 862-868, 2006.

[7] N. Nafee, S. Taetz, M. Schneider, U. F. Schaefer, and C. M. Lehr, "Chitosan-coated PLGA nanoparticles for DNA/RNA delivery: effect of the formulation parameters on complexation and transfection of antisense oligonucleotides," *Nanomedicine: Nanotechnology, Biology and Medicine,* vol. 3, pp. 173-183, 2007.

[8] J. Kim, K. V. Voelkerding, and B. K. Gale, "Patterning of a nanoporous membrane for multi-sample DNA extraction," *Journal of Micromechanics and Microengineering,* vol. 16, p. 33, 2005.

[9] T. G. Drummond, M. G. Hill, and J. K. Barton, "Electrochemical DNA sensors," *Nature Biotechnology,* vol. 21, pp. 1192-1199, 2003.

[10] J. Wang, "Electrochemical biosensors: towards point-of-care cancer diagnostics," *Biosensors and Bioelectronics,* vol. 21, pp. 1887-1892, 2006.

[11] J. Wang, "Electrochemical detection for microscale analytical systems: a review," *Talanta,* vol. 56, pp. 223-231, 2002.

[12] J. Kim and B. K. Gale, "Quantitative and qualitative analysis of a microfluidic DNA extraction system using a nanoporous AlOx membrane," *Lab Chip,* vol. 8, pp. 1516-1523, 2008.

[13] P. C. H. Li, *Microfluidic Lab-on-a-Chip for Chemical and Biological Analysis and Discovery* vol. 94: CRC, 2005.

[14] A. Liu, H. Huang, L. Chin, Y. Yu, and X. Li, "Label-free detection with micro optical fluidic systems (MOFS): a review," *Analytical and Bioanalytical Chemistry,* vol. 391, pp. 2443-2452, 2008.

[15] P. A. E. Piunno, U. J. Krull, R. H. E. Hudson, M. J. Damha, and H. Cohen, "Fiber-optic DNA sensor for fluorometric nucleic acid determination," *Analytical Chemistry,* vol. 67, pp. 2635-2643, 1995.

[16] V. Namasivayam, R. Lin, B. Johnson, S. Brahmasandra, Z. Razzacki, D. T. Burke, *et al.*, "Advances in on-chip photodetection for applications in miniaturized genetic analysis systems," *Journal of Micromechanics and Microengineering,* vol. 14, p. 81, 2003.

[17] W. Fritzsche, A. Csáki, and R. Möller, "Nanoparticle-based optical detection of molecular interactions for DNA-chip technology," in *Proceedings of SPIE*, 2002, pp. 17-22.

[18] C. Nylander, B. Liedberg, and T. Lind, "Gas detection by means of surface plasmon resonance," *Sensors and Actuators,* vol. 3, pp. 79-88, 1983.

[19] B. Liedberg, I. Lundström, and E. Stenberg, "Principles of biosensing with an extended coupling matrix and surface plasmon resonance," *Sensors and Actuators B: Chemical,* vol. 11, pp. 63-72, 1993.

[20] L. Zhang and D. Uttamchandani, "Optical chemical sensing employing surface plasmon resonance," *Electronics Letters,* vol. 24, pp. 1469-1470, 1988.

[21] S. Ekgasit, G. Stengel, and W. Knoll, "Concentration of dye-labeled nucleotides incorporated into DNA determined by surface plasmon resonance-surface plasmon fluorescence spectroscopy," *Analytical Chemistry,* vol. 76, pp. 4747-4755, 2004.

[22] Y. W. C. Cao, R. Jin, and C. A. Mirkin, "Nanoparticles with Raman spectroscopic fingerprints for DNA and RNA detection," *Science,* vol. 297, pp. 1536-1540, 2002.

[23] S. C. Kuo and M. P. Sheetz, "Force of single kinesin molecules measured with optical tweezers," *Science (New York, NY),* vol. 260, p. 232, 1993.

[24] R. Becker and B. S. S. Golovchenko, "Direct mechanical measurements of the elasticity of single DNA molecules by using magnetic beads," *Phys. Rev. Lett,* vol. 66, p. 3257, 1991.

[25] J. Fritz, M. Baller, H. Lang, H. Rothuizen, P. Vettiger, E. Meyer, *et al.*, "Translating biomolecular recognition into nanomechanics," *Science,* vol. 288, pp. 316-318, 2000.

[26] E. Palecek, "Oscillographic polarography of highly polymerized deoxyribonucleic acid," *Nature,* vol. 188, pp. 656-657, 1960.

[27] E. Paleček, "Adsorptive transfer stripping voltammetry: determination of nanogram quantities of DNA immobilized at the electrode surface," *Analytical Biochemistry,* vol. 170, pp. 421-431, 1988.

[28] L. Moreno-Hagelsieb, B. Foultier, G. Laurent, R. Pampin, J. Remacle, J. P. Raskin, *et al.*, "Electrical detection of DNA hybridization: three extraction techniques based on interdigitated Al/Al< sub> 2</sub> O< sub> 3</sub> capacitors," *Biosensors and Bioelectronics,* vol. 22, pp. 2199-2207, 2007.

[29] W. Cai, J. R. Peck, D. W. van der Weide, and R. J. Hamers, "Direct electrical detection of hybridization at DNA-modified silicon surfaces," *Biosensors and Bioelectronics,* vol. 19, pp. 1013-1019, 2004.

[30] A. T. Woolley, K. Lao, A. N. Glazer, and R. A. Mathies, "Capillary electrophoresis chips with integrated electrochemical detection," *Analytical Chemistry,* vol. 70, pp. 684-688, 1998.

[31] J. Hajdukiewicz, S. Boland, P. Kavanagh, A. Nowicka, Z. Stojek, and D. Leech, "Enzyme-amplified amperometric detection of DNA using redox mediating films on gold microelectrodes," *Electroanalysis,* vol. 21, pp. 342-350, 2009.

[32] C. Tung, "Electrical detection of DNA and integration with nano-fluidic channels," Ph.D. Dissertation, Princeton University, 2008.

[33] L. Wang, Q. Liu, Z. Hu, Y. Zhang, C. Wu, M. Yang, *et al.*, "A novel electrochemical biosensor based on dynamic polymerase-extending hybridization

for< i> E. coli</i> O157: H7 DNA detection," *Talanta,* vol. 78, pp. 647-652, 2009.

[34] A. Mugweru and J. F. Rusling, "Catalytic square-wave voltammetric detection of DNA with reversible metallopolymer-coated electrodes," *Electrochemistry Communications,* vol. 3, pp. 406-409, 2001.

[35] P. J. Viskari and J. P. Landers, "Unconventional detection methods for microfluidic devices," *Electrophoresis,* vol. 27, pp. 1797-1810, 2006.

[36] A. Numnuam, K. Y. Chumbimuni-Torres, Y. Xiang, R. Bash, P. Thavarungkul, P. Kanatharana, *et al.*, "Potentiometric detection of DNA hybridization," *Journal of the American Chemical Society,* vol. 130, p. 410, 2008.

[37] J. Heng, V. Dimitrov, Y. Grinkova, C. Ho, T. Kim, D. Muller, *et al.*, "The detection of DNA using a silicon nanopore," in *Electron Devices Meeting, 2003. IEDM'03 Technical Digest. IEEE International*, 2003, pp. 32.2. 1-32.2. 4.

[38] I. Vlassiouk, P. Takmakov, and S. Smirnov, "Sensing DNA hybridization via ionic conductance through a nanoporous electrode," *Langmuir,* vol. 21, pp. 4776-4778, 2005.

[39] M. Wanunu, J. Sutin, and A. Meller, "DNA profiling using solid-state nanopores: detection of DNA-binding molecules," *Nano letters,* vol. 9, pp. 3498-3502, 2009.

[40] P. T. Kissinger and A. Bott, "Electrochemistry for the non-electrochemist," *Current Separations,* vol. 20, pp. 51-54, 2002.

[41] B. K. Gale, K. D. Caldwell, and A. B. Frazier, "Electrical conductivity particle detector for use in biological and chemical micro-analysis systems," in *Proc. SPIE Symposium on Micromachining and Microfabrication: Micro Fluidic Devices and Systems*, 1998, pp. 230-242.

[42] A. K. Rao, "Preparation and characterization of macroporous electrodes for electrochemical bioassays," Ph.D. Dissertation, Clemson University, 2008.

[43] F. Jelen, B. Yosypchuk, A. Kourilová, L. Novotný, and E. Paleček, "Label-free determination of picogram quantities of DNA by stripping voltammetry with solid copper amalgam or mercury electrodes in the presence of copper," *Analytical Chemistry,* vol. 74, pp. 4788-4793, 2002.

[44] R. D. O'Neill, S. C. Chang, J. P. Lowry, and C. J. McNeil, "Comparisons of platinum, gold, palladium and glassy carbon as electrode materials in the design of biosensors for glutamate," *Biosensors and Bioelectronics,* vol. 19, pp. 1521-1528, 2004.

[45] X. Wang and S. Smirnov, "Label-free DNA sensor based on surface charge modulated ionic conductance," *ACS Nano,* vol. 3, p. 1004, 2009.

[46] J. Kim and A. Gonzalez-Martin, "Nanopore membrane-based electrochemical immunoassay," *Journal of Solid State Electrochemistry,* vol. 13, pp. 1037-1042, 2009.

[47] P. Kohli, M. Wirtz, and C. R. Martin, "Nanotube membrane based biosensors," *Electroanalysis,* vol. 16, pp. 9-18, 2004.

[48] F. Stuer-Lauridsen and J. Kjølholt, "Identification of selected hydrophobic organic contaminants in wastewater with semipermeable membrane devices (SPMDs)," *Water Research,* vol. 34, pp. 3478-3482, 2000.

[49] T. Gotoh, H. Iguchi, and K. I. Kikuchi, "Separation of glutathione and its related amino acids by nanofiltration," *Biochemical Engineering Journal,* vol. 19, pp. 165-170, 2004.

[50] J. Kim, K. V. Voelkerding, and B. Gale, "Multi-DNA extraction chip based on an aluminum oxide membrane integrated into a PDMS microfluidic structure," in *Microtechnology in Medicine and Biology, 2005. 3rd IEEE/EMBS Special Topic Conference*, 2005, pp. 5-7.

[51] S. Tsai, C. Chao, C. Lee, X. Liu, I. Lin, and H. Shiha, "Formation and field-emission of carbon nanofiber films on metallic nanowire arrays," *Electrochemical and Solid-State Letters,* vol. 2, pp. 247-250, 1999.

[52] X. Zhang, L. D. Zhang, W. Chen, G. W. Meng, M. Zheng, L. Zhao, *et al.*, "Electrochemical fabrication of highly ordered semiconductor and metallic nanowire arrays," *Chemistry of Materials,* vol. 13, pp. 2511-2515, 2001.

[53] F. J. Alguacil and P. Navarro, "Permeation of cadmium through a supported liquid membrane impregnated with Cyanex 923," *Hydrometallurgy,* vol. 61, pp. 137-142, 2001.

[54] S. Kentish and G. Stevens, "Innovations in separations technology for the recycling and re-use of liquid waste streams," *Chemical Engineering Journal,* vol. 84, pp. 149-159, 2001.

[55] I. Vlassiouk, F. Rios, S. A. Vail, D. Gust, and S. Smirnov, "Electrical conductance of hydrophobic membranes or what happens below the surface," *Langmuir,* vol. 23, pp. 7784-7792, 2007.

[56] M. Rhee and M. A. Burns, "Nanopore sequencing technology: research trends and applications," *Trends in Biotechnology,* vol. 24, p. 580, 2006.

[57] A. W. Smith, "Process for producing an anodic aluminum oxide membrane", U.S. Patent 3 850 762, Nov. 26, 1974.

[58] A. Thormann, N. Teuscher, M. Pfannmöller, U. Rothe, and A. Heilmann, "Nanoporous aluminum oxide membranes for filtration and biofunctionalization," *Small,* vol. 3, pp. 1032-1040, 2007.

[59] M. Tomozawa and R. H. Doremus, "Treatise on Materials Science and Technology: Vol. 26, Glass IV," 1985.

[60] R. Furneaux, W. Rigby, and A. Davidson, "The formation of controlled-porosity membranes from anodically oxidized aluminium," *Nature,* vol. 337, pp. 147-149, 1989.

[61] O. Jessensky, F. Muller, and U. Gosele, "Self-organized formation of hexagonal pore arrays in anodic alumina," *Applied Physics Letters,* vol. 72, pp. 1173-1175, 1998.

[62] M. C. Breadmore, K. A. Wolfe, I. G. Arcibal, W. K. Leung, D. Dickson, B. C. Giordano, *et al.*, "Microchip-based purification of DNA from biological samples," *Analytical Chemistry,* vol. 75, pp. 1880-1886, 2003.

[63] H. H. Kessler, G. Mühlbauer, E. Stelzl, E. Daghofer, B. I. Santner, and E. Marth, "Fully automated nucleic acid extraction: MagNA Pure LC," *Clinical Chemistry,* vol. 47, pp. 1124-1126, 2001.

[64] Y. Ye and H. Ju, "DNA electrochemical behaviors, recognition and sensing by combining with PCR technique," *Sensors,* vol. 3, pp. 128-145, 2003.

[65] K. Hashimoto, K. Ito, and Y. Ishimori, "Microfabricated disposable DNA sensor for detection of hepatitis B virus DNA," *Sensors and Actuators B: Chemical,* vol. 46, pp. 220-225, 1998.

[66] Y. D. Zhao, D. W. Pang, S. Hu, Z. L. Wang, J. K. Cheng, and H. P. Dai, "DNA-modified electrodes; part 4: optimization of covalent immobilization of DNA on self-assembled monolayers," *Talanta,* vol. 49, pp. 751-756, 1999.

[67] A. Ferancová, M. Adamovski, P. Gründler, J. Zima, J. Barek, J. Mattusch, *et al.*, "Interaction of tin (II) and arsenic (III) with DNA at the nanostructure film modified electrodes," *Bioelectrochemistry,* vol. 71, pp. 33-37, 2007.

[68] Y. Mishima, J. Motonaka, K. Maruyama, I. Nakabayashi, and S. Ikeda, "Glucose sensor based on titanium dioxide electrode modified with potassium hexacyanoferrate (III)," *Sensors and Actuators B: Chemical,* vol. 65, pp. 343-345, 2000.

[69] I. Moser, G. Jobst, and G. A. Urban, "Biosensor arrays for simultaneous measurement of glucose, lactate, glutamate, and glutamine," *Biosensors and Bioelectronics,* vol. 17, pp. 297-302, 2002.

[70] M. A. T. Gilmartin and J. P. Hart, "Sensing with chemically and biologically modified carbon electrodes. A review," *Analyst,* vol. 120, pp. 1029-1045, 1995.

[71] M. Pedano and G. Rivas, "Immobilization of DNA on glassy carbon electrodes for the development of affinity biosensors," *Biosensors and Bioelectronics,* vol. 18, pp. 269-277, 2003.

[72] L. Murphy, "Biosensors and bioelectrochemistry," *Current Opinion in Chemical Biology,* vol. 10, pp. 177-184, 2006.

[73] F. Jelen, A. Kouřilová, P. Pečinka, and E. Paleček, "Microanalysis of DNA by stripping transfer voltammetry," *Bioelectrochemistry,* vol. 63, pp. 249-252, 2004.

[74] R. Kizek, L. Havran, M. Fojta, and E. Paleček, "Determination of nanogram quantities of osmium-labeled single stranded DNA by differential pulse stripping voltammetry," *Bioelectrochemistry,* vol. 55, pp. 119-121, 2002.

[75] M. Fojta, L. Havran, M. Vojtiskova, and E. Palecek, "Electrochemical detection of DNA triplet repeat expansion," *Journal of the American Chemical Society,* vol. 126, pp. 6532-6533, 2004.

[76] D. H. Johnston and H. H. Thorp, "Cyclic voltammetry studies of polynucleotide binding and oxidation by metal complexes: homogeneous electron-transfer kinetics," *The Journal of Physical Chemistry,* vol. 100, pp. 13837-13843, 1996.

[77] X. Zhao, Z. Mai, X. Kang, and X. Zou, "Direct electrochemistry and electrocatalysis of horseradish peroxidase based on clay–chitosan-gold nanoparticle nanocomposite," *Biosensors and Bioelectronics,* vol. 23, pp. 1032-1038, 2008.

[78] L. Trnková, "Electrochemical behavior of DNA at a silver electrode studied by cyclic and elimination voltammetry," *Talanta,* vol. 56, pp. 887-894, 2002.

[79] L. Trnková, R. Kizek, and O. Dračka, "Elimination voltammetry of nucleic acids on silver electrodes," *Bioelectrochemistry,* vol. 55, pp. 131-133, 2002.